NMR shifts for polycyclic aromatic hydrocarbons from first-principles

T. Thonhauser,[1] Davide Ceresoli,[2] and Nicola Marzari[2]

[1]*Department of Physics, Wake Forest University, Winston-Salem, North Carolina 27109, USA.*
[2]*Department of Materials Science and Engineering, MIT, Cambridge, Massachusetts 02139, USA.*

(Dated: September 3, 2009)

We present first-principles, density-functional theory calculations of the NMR chemical shifts for polycyclic aromatic hydrocarbons, starting with benzene and increasing sizes up to the one- and two-dimensional infinite limits of graphene ribbons and sheets. Our calculations are performed using a combination of the recently developed theory of orbital magnetization in solids, and a novel approach to NMR calculations where chemical shifts are obtained from the derivative of the orbital magnetization with respect to a microscopic, localized magnetic dipole. Using these methods we study on equal footing the ^{1}H and ^{13}C shifts in benzene, pyrene, coronene, in naphthalene, anthracene, naphthacene, and pentacene, and finally in graphene, graphite, and an infinite graphene ribbon. Our results show very good agreement with experiments and allow us to characterize the trends for the chemical shifts as a function of system size.

PACS numbers: 71.15.-m, 71.15.Mb, 75.20.-g, 76.60.Cq

I. INTRODUCTION

The experimental technique of nuclear magnetic resonance (NMR) has been known since the 1930's,[1] and has since become one of the most widely used methods in structural chemistry.[2] Along with experimental advancements over the several past decades, it was soon realized that ab-initio calculations could greatly aid in unambiguously determining structures from NMR spectra. Such calculations were first developed in the quantum-chemistry community;[3] however, these developments applied only to finite systems, such as molecules and clusters. Application to extended systems is hindered by the difficulty of including macroscopic magnetic fields, which require a non-periodic vector potential and therefore destroy Bloch symmetry. This shortcoming was overcome by Mauri *et al.*, who developed a linear-response approach for calculating NMR shieldings in periodic crystals based on the long-wavelength limit of a periodic modulation of the applied magnetic field.[4] Similarly, Sebastiani and Parrinello used the Wannier representation to derive an alternative linear-response approach based on the application of an infinitesimal uniform magnetic field.[5] In recent years these approaches have been advanced and refined,[6–8] leading to a growing use in modern plane-wave pseudopotential codes.[9–11] Nevertheless, the linear-response framework central to all these approaches makes them fairly complex and difficult to implement.

We have recently developed a novel method to calculate chemical shifts in periodic systems,[12] where the need for a linear-response framework is circumvented by construction. While early results for simple molecules and hydrocarbons provided a proof of principle for our approach,[12] albeit limited to hydrogen shifts, we apply it here systematically to calculate chemical shifts for both hydrogen and carbon in polycyclic aromatic hydrocarbons (PAH). Starting from benzene, we will explore the one-dimensional and two-dimensional progression that include either pyrene and coronene on one side, or naphthalene, anthracene, etc., until we reach the infinite limits represented by graphene (and, by extension, graphite), or graphene ribbons.

We focus this study on PAHs because of the recent surge of interest in energy related materials and their impact on environmental and health issues. PAHs occur in fossil fuels such as oil and coal, and they are a byproduct of incomplete combustion in e.g. wood, fat, tobacco, or incense. Depending on structure, these pollutants can be extremely toxic, carcinogenic, mutagenic, and teratogenic. It is thus not surprising that in recent years NMR techniques have been developed to determine the content of PAHs in our environment.[13] A tool combining ab-initio information with experimental techniques might lead to more efficient and precise devices for detecting PAHs in e.g. soil or air.

This paper is organized in the following way: For completeness we present in Sec. II a short theory summary of our converse approach to NMR shifts. Details about our numerical calculations and about the practical implementation of the converse method can be found in Sec. III. Results for finite PAHs are presented in Sec. IV A, whereas results for periodic systems are collected in Sec. IV B. We will conclude and summarize in Sec. V.

II. THEORY

The usual approach to calculating NMR shifts in periodic systems is to apply a magnetic field and calculate the local field at the nucleus using a linear-response framework. We will refer to this approach as *direct*, since it computes the shifts directly from the applied and induced fields. Since a constant field is not compatible with periodic-boundary conditions, the approach developed by the solid-state community has been to use linear-response theory in the limit of long-wavelength perturbations.[4] We recently argued that it is actually possible to calculate the

shifts in periodic systems without using a linear-response framework. In our *converse* approach we circumvent the linear-response framework in that we relate the shifts to the macroscopic magnetization induced by magnetic point dipoles placed at the nuclear sites of interest. We report here the essential result and refer the reader to Ref. [12] for details.

We define E as the energy of a virtual magnetic dipole $\mathbf{m}_s$ at one nuclear center $\mathbf{r}_s$ in the field $\mathbf{B}$ for a finite system, or as the energy per cell of a periodic lattice of such dipoles. Then, writing the macroscopic magnetization as $M_\beta = -\Omega^{-1}\,\partial E/\partial B_\beta$ (where Ω is the cell volume),

$$\delta_{\alpha\beta} - \sigma_{s,\alpha\beta} = -\frac{\partial}{\partial B_\beta}\frac{\partial E}{\partial m_{s,\alpha}} = -\frac{\partial}{\partial m_{s,\alpha}}\frac{\partial E}{\partial B_\beta} = \Omega\frac{\partial M_\beta}{\partial m_{s,\alpha}}\ . \tag{1}$$

It follows that $\overleftrightarrow{\sigma}_s$ accounts for the shielding contribution to the macroscopic magnetization induced by a magnetic point dipole $\mathbf{m}_s$ sitting at nucleus $\mathbf{r}_s$ and all of its periodic replicas. Instead of applying a constant (or long-wavelength) field $\mathbf{B}^{\text{ext}}$ to an infinite periodic system and calculating the induced field at all equivalent s nuclei, we apply an infinite array of magnetic dipoles to all equivalent sites s, and calculate the change in magnetization. Since the perturbation is now periodic, it can simply be computed using finite differences of ground-state calculations. Note that $\mathbf{M} = \mathbf{m}_s/\Omega + \mathbf{M}^{\text{ind}}$, where the first term is present merely because we have included magnetic dipoles by hand. The shielding is related to the true induced magnetization via $\sigma_{s,\alpha\beta} = -\Omega\,\partial M^{\text{ind}}_\beta/\partial m_{s,\alpha}$.

NMR is a technique that probes for properties of the electronic structure near the nuclei. Thus, a good description of the wave functions near the nuclei is vital. The formalism described above can directly be implemented into all-electron programs such as LAPW codes. However, many codes use plane waves as a basis and the ionic potential is replaced by a pseudopotential to keep the computational cost low. In these cases, extra care has to be taken when calculating NMR shifts. While hydrogen shifts can be described correctly using Coulombic (pseudo)potentials, a reconstruction of the pseudovalence wave functions in the core region has to be performed for elements beyond the first row.[4] This can be achieved with the so called gauge-including projector augmented-wave (GIPAW) method, which has been developed by Pickard and Mauri in 2001 and proved very efficient for NMR calculations using pseudopotentials.[7] We have derived the corresponding GIPAW formalism for the converse method, but the lengthy, mathematical details will be presented in a forthcoming article.[14]

III. IMPLEMENTATION AND CALCULATIONAL DETAILS

We have implemented the converse method outlined above into the plane-wave density functional theory code PWSCF, which is part of the Quantum-ESPRESSO distribution.[15] We added an extra term to the Hamiltonian taking into account the electron orbital interaction with a nuclear magnetic dipole $\mathbf{m}_s$ sitting at nucleus $\mathbf{r}_s$, by the usual substitution for the momentum operator $\mathbf{p} \to \mathbf{p} + \frac{e}{c}\mathbf{A}$, where $\mathbf{A}$ is the vector potential of a periodic array of nuclear dipoles. This is done conveniently in reciprocal space and requires only a few dozen lines of additional code. The calculation and implementation of the orbital magnetization[16–20] necessary to evaluate Eq. (1) is somewhat more involved. However, a growing number of codes has the calculation of the orbital magnetization already implemented so that the NMR shifts can be calculated readily. Also, if one is only interested in finite systems, one can calculate the induced magnetic moment instead of the orbital magnetization, which is much simpler (the moment can be calculated from the quantum-mechanical current, which requires only knowledge of the wave functions). Since we are interested in shifts of atoms other than hydrogen, we also implemented a GIPAW reconstruction, as mentioned above.

It might appear that the converse method is computationally demanding, since we need to perform $3N$ calculations to obtain the shielding tensor for N atoms. However, note that in practice a single full self-consistent ground-state calculation is performed once, and then the dipole perturbations according to each shielding are applied to this ground state. Convergence after the perturbation is much faster than the ground-state calculation, and we find that NMR shifts for systems with hundreds of atoms can be easily calculated.

For our calculations in the following sections we have used a PBE exchange-correlation functional and norm-conserving pseudopotentials of the Troullier-Martins type[21] with a cutoff of 80 Rydberg. The structural parameters of all systems have been optimized within this framework. For the dipole perturbation we chose a value of $|\mathbf{m}_s|$ of $1\mu_{\text{B}}$, although the results are independent of the exact value over a wide range.

In order to compare the accuracy of our converse method to the direct method, we performed test calculations on benzene and diamond. For the finite system benzene using the converse method we find an absolute hydrogen shielding of 22.97 ppm and carbon shielding of −165.2 ppm. These results compare well with the results obtained using the direct method: 22.69 ppm and −163.4 ppm. For periodic diamond we find a shielding of −63.89 ppm compared to the direct method which gives −65.85 ppm.[6] Note that in all cases the carbon shielding includes only the shielding from the valence electrons and does not include the core shielding, which we calculate to be +200.3 ppm. The small deviations between the converse and the direct method are most likely due to the fact that the direct method uses a linear-response framework in which a finite q-vector is used to make the magnetic field periodic and modulate it over space, instead of using a truly constant magnetic field.

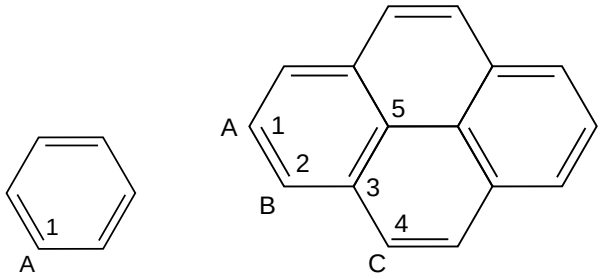

FIG. 1: Schematic model of benzene (left) and pyrene (right). In order to refer to certain atoms and their NMR shift, we use the labeling shown. In general, hydrogen atoms are label by letters, whereas carbon atoms are labeled by numerals.

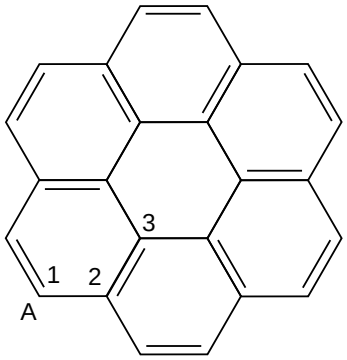

FIG. 2: Schematic model of coronene.

IV. RESULTS

NMR experiments usually report the isotropic shielding $\sigma_s = \frac{1}{3}\mathrm{Tr}[\overleftrightarrow{\sigma}_s]$ via the chemical shift $\delta_s = -(\sigma_s - \sigma_{\mathrm{ref}})$. Here σ_{ref} is the isotropic shielding of a reference compound such as tetramethylsilane (TMS). Note that we have not calculated the shielding of TMS itself, however, we can still report shifts with respect to TMS by using our calculations for e.g. benzene as an intermediate reference: $\delta_s = -(\sigma_s - \sigma_{\mathrm{calc}}^{\mathrm{benzene}} - \delta_{\mathrm{TMS}}^{\mathrm{benzene}})$. For $\delta_{\mathrm{TMS}}^{\mathrm{benzene}}$ we have used the experimental values of 128.6 ppm for carbon and 7.26 ppm for hydrogen.[22] Henceforth, we will use the notation $\delta_s^{\mathrm{molecule}}$ to describe the shift relative to TMS of atom s in a certain molecule. We will use letters $s = A, B, C, \ldots$ to refer to hydrogen shifts and numerals $s = 1, 2, 3, \ldots$ for carbon shifts.

A. Finite systems

We start out by calculating the ^{1}H and ^{13}C NMR shifts of several small PAHs. We start with benzene, and move towards the one-dimensional limit by adding one ring at a time, to study naphthalene, anthracene, naphthacene, and pentacene. The two-dimensional limit is considered via pyrene and coronene, i.e. surrounding benzene by more rings in the plane. For all these calculations we used a large supercell with at least 16 Bohr of vacuum between periodic replicas. Note that the magnetic susceptibility of these systems effectively vanishes and our computed shifts can be directly compared to the experimental ones without any shape correction.[23]

Our results for pyrene and coronene are collected in Table I. For a definition of their atomic positions see Figs. 1 and 2. In general, we find very good agreement between the experimental results and our calculations. The small deviations are most likely due to the approximative nature of DFT with respect to the exchange and correlation functional. Using e.g. the local-density approximation for the exchange-correlation functional, we get slightly different results. However, a detailed and comprehensive study is necessary to adequately investigate the effect of the functional used on the NMR shifts.[26] In principle, since we are calculating the shift through the orbital magnetization, which is closely related to electrical currents, it might be more appropriate to use a current-density functional rather than one of the standard density-only functionals. Unfortunately, appropriate current-density functionals (e.g. Ref. [27]) are not yet available in most DFT codes. Note that the relative shifts (that is, the difference in shift between different atoms) are closely reproduced. This is important, as relative shifts play the key role in linking NMR data to a structure.

As one would expect, all shifts of pyrene and coronene are significantly different from the pure benzene shifts. However, it is interesting to see that the hydrogen shifts increase, while all carbon shifts decrease—except one. It is $\delta_3^{\mathrm{pyrene}}$ and $\delta_2^{\mathrm{coronene}}$ that rise above the 128.6 ppm of benzene. These shifts both correspond to carbon atoms

TABLE I: Hydrogen and carbon NMR chemical shifts in ppm for pyrene and coronene. For a definition of atomic positions see Figs. 1 and 2. Note that we have used the shifts of benzene as a reference.

Molecule	atom	experiment	calculation
Benzene	1	128.6 [a]	—
	A	7.26 [a]	—
Pyrene	1	125.5 [a]	122.2
	2	124.6 [a]	122.1
	3	130.9 [a]	130.4
	4	127.0 [a]	126.0
	5	124.6 [a]	123.4
	A	7.60–8.15 [b]	8.61
	B	7.60–8.15 [b]	8.57
	C	7.60–8.15 [b]	8.47
Coronene	1	126.2 [a]	123.5
	2	128.7 [a]	129.3
	3	122.6 [a]	122.6
	A	8.89 [c]	9.78

[a] Reference [22].
[b] Reference [24].
[c] Reference [25].

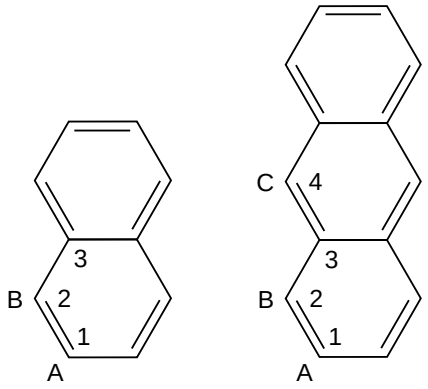

FIG. 3: (**left**) Naphthalene. (**right**) Anthracene.

TABLE II: Hydrogen and carbon NMR chemical shifts in ppm for naphthalene and anthracene. For a definition of atomic positions see Fig. 3.

Molecule	atom	experiment	calculation
Benzene	1	128.6 [a]	—
	A	7.26 [a]	—
Naphthalene	1	125.7 [c]	123.0
	2	127.8 [c]	126.2
	3	133.4 [c]	133.1
	A	7.41 [b]	8.08
	B	7.79 [b]	8.13
Anthracene	1	126.1 [c]	125.0
	2	128.1 [c]	127.8
	3	131.6 [c]	132.0
	4	125.3 [c]	121.6
	A	7.41 [b]	7.95
	B	7.95 [b]	8.24
	C	8.40 [b]	8.44

[a] Reference [22].
[b] Reference [24].
[c] Reference [25].

that have no hydrogens attached.

Our results for the one-dimensional chains from naphthalene to pentacene are given in Tables II and III. For a definition of the corresponding atomic positions see Figs. 3 and 4. As before, we find very good agreement between the experimental results and our calculations. The exact same statements concerning the differences compared to benzene apply: hydrogen shifts increase, while carbon shifts decrease—expect one. In these chains it is the carbon shift of atom 3 that increases, which again corresponds to a carbon that is not connected to a hydrogen.

Note that we have not included experimental results for naphthacene and pentacene. Although there are some results reported (see e.g. Ref. [28]) these molecules are insoluble in most of the solvents used for the preparation

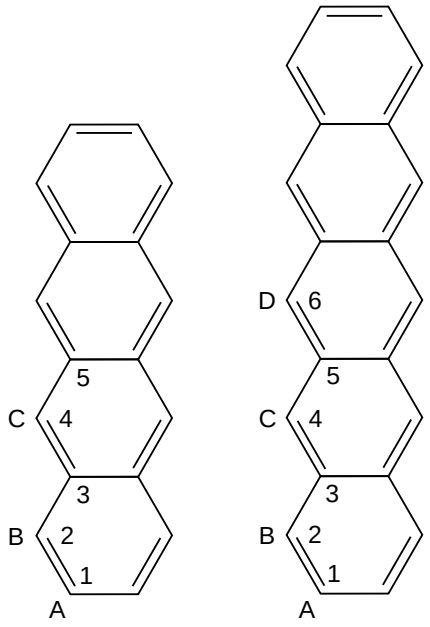

FIG. 4: (**left**) Naphthacene. (**right**) Pentacene.

TABLE III: Hydrogen and carbon NMR chemical shifts in ppm for naphthacene and pentacene. For a definition of atomic positions see Fig. 4.

Naphthacene		Pentacene	
atom	calc.	atom	calc.
1	122.3	1	123.3
2	126.5	2	127.4
3	130.5	3	130.6
4	125.5	4	125.0
5	128.1	5	128.5
A	8.31	6	125.4
B	8.68	A	8.37
C	9.07	B	8.74
		C	9.21
		D	9.46

of NMR cuvettes.

B. Periodic systems

The systems discussed above can systematically be expanded until they eventually become infinite. In a one-dimensional way, we extend the chains naphthalene, anthracene, naphthacene, pentacene, ... until we reach an infinite ribbon. On the other hand, if we extend pyrene and coronene in a two-dimensional way, we arrive at graphene. Stacking graphene sheets on top of each other yields graphite.

We have calculated the hydrogen and carbon shifts for these extended systems. These infinite systems show

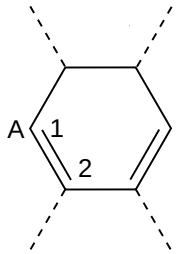

FIG. 5: Section of an infinite ribbon consisting of benzene rings.

metallic behavior and therefore require a dense k-point mesh. For our calculations we have used up to 16 k-points in the directions of periodicity and a gaussian smearing of 0.001 Rydberg to obtain converged results. As another result of the metallic behavior, Knight shifts might influence the NMR spectrum. While schemes do exist to calculate Knight shifts within plane-wave DFT approaches,[29] we did not include them in our calculations.

For graphene we find a carbon shift of 118.0 ppm. The two in-equivalent carbon shifts in graphite give 124.3 ppm and 134.9 ppm. For the infinite ribbon depicted in Fig. 5 we find $\delta_A^{\rm ribbon}$=8.56 ppm, $\delta_1^{\rm ribbon}$=128.0 ppm, and $\delta_2^{\rm ribbon}$=132.2 ppm. Experimentally, solid state NMR spectra of graphite show a broad peak in the range 155÷179 ppm, depending on sample preparation. This broadening is due to a fairly long lattice relaxation time T_1 and the presence of conduction electrons.[30]

In order to compare our results for graphite with experimental data, in principle one would have to include a shape correction involving the susceptibility.[23] This correction is estimated to be of the order of 1÷2 ppm in most forms of graphite sample such as powder samples. The only exception is highly oriented pyrolytic graphite, which has a very large and anisotropic magnetic susceptibility, where the shape correction is expected to be of the order of 10÷20 ppm.

The calculated shifts for these periodic systems are interesting in and of themselves. However, we now want to focus on the change in shift as the systems grow larger and eventually become infinite. One would expect to find a correlation between the shifts in finite and infinite systems. Indeed, looking at the carbon shifts we find $\delta_1^{\rm benzene} \rightarrow \delta_5^{\rm pyrene} \rightarrow \delta_3^{\rm coronene} \rightarrow \delta^{\rm graphene}$ with the results 128.6 → 123.4 → 122.6 → 118.0 ppm. Although NMR is a local probe, it turns out that the size of coronene is not yet big enough for its bulk atoms to behave like graphene.

If we start at benzene again and add rings in a liner fashion, we can grow a chain of arbitrary length. Looking at the carbon shifts we find the sequence $\delta_4^{\rm anthracene} \rightarrow \delta_6^{\rm pentacene} \rightarrow \delta_1^{\rm ribbon}$ with the corresponding results 121.6 → 125.4 → 128.0 ppm. As with the graphene sheet, this result suggests that a finite chain would need to be longer than pentacene so that its carbon atoms behave like an infinite ribbon. Looking at sequences that end at $\delta_A^{\rm ribbon}$ or $\delta_2^{\rm ribbon}$, no clear trend is visible.

V. CONCLUSIONS

We have used an alternative first-principles method to calculate NMR chemical shifts of a variety of polycyclic aromatic hydrocarbons and related infinite systems. Our results are in good agreement with experiment. By going from finite to periodic systems, we observe trends in shifts which suggest that neither coronene nor pentacene are large enough to model their infinite counterparts.

In future work we would like to include the shifts of other PAHs as well as study the Knight shifts of graphene.

VI. ACKNOWLEDGMENTS

We are grateful for extensive discussions with F. Mauri. This work was supported by NSF grant DMR-0549198, ONR grant N00014-07-1-1095, and the DOE/SciDAC project on Quantum Simulation of Materials and Nanostructures.

[1] Rabi, I. I.; Zacharias, J. R.; Millman, S.; Kusch, P. Phys Rev 1938, 53, 318.
[2] Encyclopedia of NMR; Grant, D.M.; Harris, R.K., Eds.; Wiley: London, 1996.
[3] Kutzelnigg, W.; Fleischer, U; Schindler, M. NMR Basic Principles and Progress; Springer: Berlin, 1990.
[4] Mauri, F.; Pfrommer, B. G.; Louie, S. G. Phys Rev Lett 1996, 77, 5300.
[5] Sebastiani, D.; Parrinello, M. J Phys Chem A 2001, 105, 1951.
[6] Pickard, C. J.; Mauri, F. Phys Rev B 2001, 63, 245101.
[7] Pickard, C. J.; Mauri, F. Phys Rev Lett 2003, 91, 196401.
[8] Yates, J. R.; Pickard, C. J.; Mauri, F. Phys Rev B 2007, 76, 024401.
[9] Pfrommer, B. G.; Demmel, J.; Simon, H. J Comp Phys 1999, 150, 287.
[10] Pfrommer, B. G.; Coté, M.; Louie, S. G.; Cohen, M. L. J Comp Phys 1997, 131, 233.
[11] Clark, S. J.; Segall, M. D.; Pickard, C. J.; Hasnip, P. J.; Probert, M. J.; Refson, K.; Payne, M. C. Zeitschrift für Kristallographie 2005, 220(5-6), 567.
[12] Thonhauser, T.; Mostofi, A.; Marzari, N.; Resta, R.; Vanderbilt, D. arXiv:0709.4429, unpublished.
[13] Weisshoff, H.; Preiss, A.; Nehls, I.; Win, T.; Muegge, C. Anal Bioanal Chem 2002, 373, 810.
[14] Ceresoli, D.; Thonhauser, T.; Marzari, N. unpublished.

[15] Baroni, S.; *et al.*, http://www.quantum-espresso.org.

[16] Resta, R.; Ceresoli, D.; Thonhauser, T.; Vanderbilt, D. ChemPhysChem 2005, 6, 1815.

[17] Thonhauser, T.; Ceresoli, D.; Vanderbilt, D.; Resta, R. Phys Rev Lett 2005, 95, 137205.

[18] Ceresoli, D.; Thonhauser, T.; Vanderbilt, D.; Resta, R. Phys Rev B 2006, 74, 24408.

[19] Ceresoli, D.; Resta, R. Phys Rev B 2007, 76, 012405.

[20] Shi, J.; Vignale, G.; Xiao, D.; Niu, Q. Phys Rev Lett 2007, 99, 197202.

[21] Troullier N.; Martins, J. L. Phys Rev B 1991, 43, 1993.

[22] Landolt–Börnstein – Group III Condensed Matter; Gupta, R. R.; Lechner, M. D., Eds.; Springer: New York; Vol. 35, 2005.

[23] It can be shown that the shielding for a general shape is related to our calculated one by $\sigma^{\rm shape}_{s,\alpha\beta} \simeq \sigma_{s,\alpha\beta} - \delta_{\alpha\beta}\, 4\pi\chi(1-n_\beta)$, where n_α are the depolarization coefficients (with $\sum_\alpha n_\alpha = 1$) and χ is the magnetic susceptibility χ.

[24] The Sadtler Handbook of Proton NMR Spectra; Simons, W. W., Ed., Sadtler Research Laboratories Inc.: Philadelphia; 1978.

[25] Pouchert C. J.; Behnke, J. The Aldrich Library of ^{13}C and ^{1}H FT NMR Spectra; Aldrich Chemical Company Inc.: publisher, 1993.

[26] Zhao Y.; Truhlar, D. G. J Phys Chem 2008, 112, 6794.

[27] Vignale, G.; Rasolt, M. Phys Rev Lett 1987, 59, 2360.

[28] Nagano, M.; Hasegawa, T.; Myoujin, N.; Yamaguchi, J.; Itaka, K.; Fukumoto, H.; Yamamoto, T.; Koinuma, H. Jpn J Appl Phy 2004, 43, L315.

[29] d'Avezac, M.; Marzari, N.; Mauri, F. Phys Rev B 2007, 76, 165122.

[30] Suganuma, M.; Mizutami, U.; Kondow, T. Phys Rev B 1980, 22, 5079.